MF R-Mode 2-Channel Receiver and Skywave Report

31 March 2017

Prepared by:

Alion Science & Technology
1 Chelsea St., Ste. 200
New London, CT 06320

PI: Dr. Gregory W. Johnson

ALION
SCIENCE AND TECHNOLOGY

Executive Summary

Position, Navigation, and Timing (PNT) is part of the critical infrastructure necessary for the safety and efficiency of vessel movements, especially in congested areas such as the North Sea. Global Navigation Satellite Systems (GNSS), especially the U.S. Global Positioning System (GPS), have become the primary PNT sources for maritime operations. The GNSS position is used both for vessel navigation and as the position and timing source for other systems such as Automatic Identification System (AIS).

Unfortunately, GNSS is vulnerable to jamming and interference, intentional or not, which can lead to the loss of positioning information or, even worse, to incorrect positioning information. The user requirement is for dependable PNT information at all times. One potential source of resilient PNT services is Ranging Mode (R-Mode), an alternative PNT concept related to Signals of OPportunity (SoOP) PNT, which uses signals independent of GNSS.

In 2013 the German Federal Waterways and Shipping Administration contracted for a feasibility study of R-Mode using medium frequency (MF) Differential GNSS (DGNSS) and very high frequency (VHF) AIS signals as well as those signals in combination and in combination with eLoran. At ION GNSS+ 2014 we presented the results from that feasibility study and showed the projected performance using the signals individually and in combination. In most of the shipping lanes on the North Sea it appeared that 10m or better performance could be achieved.

Following up on that work, prototypes of a transmitter and receiver for MF-DGNSS R-Mode have been developed. The transmitter was installed in IJmuiden (Netherlands) and the receiver deployed along the Dutch coast to the south of the transmitter for initial on-air testing of the R-Mode concept; both were synchronized to UTC via GPS. While positioning is not possible with only one R-Mode transmitter, the combination of a synchronized transmitter and receiver pair allows for useful testing of the R-Mode concept. Specifically, the receiver could estimate a true range (rather than a pseudorange); hence, the stability of the range with environmental variations (e.g. weather, day/night skywave effects, etc.) can be studied.

To further study skywave effects, the R-Mode modulator was relocated to a more powerful transmitter at Heligoland (Germany) and the receiver moved to a location near the Kiel Canal (Germany). A second receiver was installed at a similar distance from the transmitter to enable simultaneous comparison of two different propagation paths. Later a third receiver was added in order to provide three paths of different lengths.

This report presents details of the prototype transmitter and receiver and includes statistical analyses of the range estimates recorded to date and the impact of skywave interference at night using data from the German test sites.

Table of Contents

List of Figures

1. INTRODUCTION

Position, Navigation, and Timing (PNT) is part of the critical infrastructure necessary for the safety and efficiency of vessel movements, especially in congested areas such as the North Sea. Global Navigation Satellite Systems (GNSS), especially the U.S. Global Positioning System (GPS), have become the primary PNT sources for maritime operations. The GNSS position is used both for vessel navigation and as the position and timing source for other bridge systems, such as Automatic Identification System (AIS). Unfortunately, GNSS is vulnerable to jamming and interference, whether intentional or not, which can lead to the loss of positioning information or, even worse, to incorrect positioning information. The user requirement is for dependable PNT information at all times, even under GNSS jamming conditions. A variety of technological solutions to an alternative PNT system are possible; in the radio frequency (RF) domain we have the so-called "Signals of OPportunity" (SoOP) approach (e.g. [1]). This term refers to the opportunistic use of RF signals, typically communications signals, which exist in the geographical area of the receiver. While these signals are not primarily intended for positioning, a SoOP navigation receiver attempts to exploit them as such. Specifically, if each SoOP can provide a (pseudo) range to the receiver from a known location, a trilateration position solution is possible. Usually, there is no alteration of the SoOP signal. In some instances, minor improvements are initiated to improve the signal's characteristics; for example, synchronizing the signal to a known (and GNSS independent) source of UTC. So called "Ranging Mode" (or R-Mode) is one such example.

In 2013 the German Federal Waterways and Shipping Administration contracted for a feasibility study of R-Mode using medium frequency (MF) differential GNSS (DGNSS) and very high frequency (VHF) AIS signals as well as those signals in combination and in combination with eLoran [2]. This study was part of the European Accessibility for Shipping, Efficiency Advantages and Sustainability (ACCSEAS) project. At the Institute of Navigation (ION) GNSS+ 2014 conference we presented the results from that feasibility study and showed the projected performance using the signals individually and in combination [3]. The study stated that AIS R-Mode was feasible with the existing signal structure (beyond synchronizing the broadcasts and, perhaps, adding a fixed ranging message), but that DGNSS R-Mode would be greatly improved by actually modifying the signal, adding one or two continuous wave (CW) signals to the broadcast (i.e. not be a pure SoOP, but a hybrid version). In most of the shipping lanes of the North Sea it appeared that 10-meter or better performance could be achieved via R-Mode. Rather than define desired performance up front, the approach of the ACCSEAS project was to try to identify what level of performance was possible and identify what limited the system performance. The decision could then be made as to whether the solution was worth pursuing.

To continue that work, prototypes of an MF-DGNSS R-Mode modulator and receiver were developed. The modulator was installed at a transmission site in Ijmuiden (Netherlands) and the receiver deployed to the south along the Dutch coast for initial on-air testing of the R-Mode concept. While positioning is not possible with only one R-Mode transmitter, the combination of a synchronized transmitter and receiver pair allowed for useful testing of the R-Mode concept. Specifically, having both the transmitter and receiver clocks synchronized to a common time

source (UTC via GPS in this case, noting that the final full system would be GNSS independent) allows the receiver to estimate a true range (rather than a pseudorange); hence, the stability of the range with environmental variations (e.g. weather, day/night skywave effects, etc.) could be studied. To further study propagation and skywave effects, the R-Mode modulator was relocated to a more powerful transmitter at Heligoland in the North Sea and the receiver moved to a location near the Kiel Canal (east of the transmitter). A second receiver was installed to the west of the transmitter to enable simultaneous comparison of two different propagation paths. A third receiver site, nearly along the signal propagation path to the Kiel Canal, was added most recently. After a brief description of both the modulator and receiver below, experimental results from these receivers are presented.

2. BACKGROUND ON MF DGNSS BROADCASTS

The MF DGNSS system transmits its information via a binary modulation method known as Minimum Shift Keying (MSK) [4]. Assuming that the MSK transmission is controlled by a precise time/frequency source, both the times of the bit transitions (potentially once every 10 milliseconds) and the underlying phase of the transmitted signal (a sinusoid at approximately 300 kHz) could be exploited to estimate the time of arrival (TOA) for ranging applications. The R-Mode feasibility report examined the potential performance of estimators of TOA from these two parameters [2]. It was argued that with the existing signal strengths and beacon locations, the time of bit transition is too imprecise for effective ranging. However, assuming that the cycle ambiguity could be resolved, the carrier phase could yield sufficient accuracy. Further, while this level of performance is conceptually possible with the direct MF transmission, it would be significantly easier if in-band continuous wave (CW) signals accompanied the MF and the phase of this separate CW was estimated (similar to Omega [5]). The system proposed in [2] adds two CW signals to the MSK transmission; one below and one above the MSK carrier. Nominal values for the offset in frequency from the MSK carrier are ±225 Hz (recall that the European standards for DGNSS call for a 500 Hz channel bandwidth thus limiting the offsets from the carrier frequency to less than ±250 Hz).

Ranging on the CW signals was analyzed and a bound on estimation accuracy was determined in [2, 6]. For phase estimation the Cramer-Rao lower bound on accuracy is

$$\sigma^2_{\tau\,\widehat{carrier}} \geq \frac{1}{2\omega_c{}^2 T\ SNR}\ seconds$$

in which T is the observation period, ω_c is the MF carrier frequency (in radians per second), and SNR is the received signal to noise ratio. Converting to meters and taking a square root yields the standard deviation

$$\sigma_{MF\ carrier} \geq \frac{1.2\times10^4}{\omega_c\sqrt{T\ SNR}}\ meters$$

Figure 1 shows the potential performance (measured in meters of standard deviation) as a function of signal to noise ratio (SNR) (in dB based upon predicted signal levels and typical North Sea noise values in dBμV). The lines labeled “weak” and “typical” suggest the level of performance available in the North Sea region assuming a 5-second averaging window on the estimator.

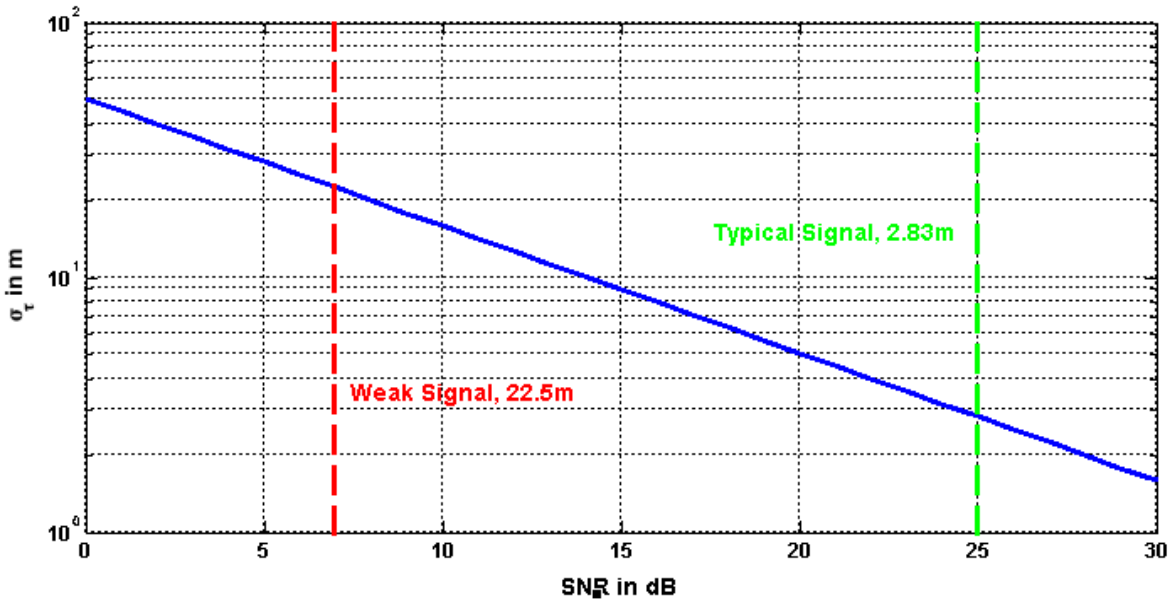

Figure 1: The Cramer-Rao lower bound on performance of estimating the time of arrival from the phase of the MF ranging signal as a function of signal to noise ratio.

There are several important points to remember for MF DGNSS ranging:

- Ranging using carrier phase requires the resolution of cycle ambiguity, the fact that the phase repeats every wavelength of the signal (this is approximately 1 km for MF DGNSS signals). CW signals allow for several ambiguity resolution approaches: (1) initializing the receiver at a fixed location and "counting" cycles as the platform moves or (2) using time synchronized, multiple frequency signals and solving for a position that simultaneously satisfies all of the ambiguity equations with integer solutions. Such solutions have been discussed since the introduction of Omega, which also used different frequencies from spatially separated transmitters (e.g. [7]).
- The propagation of an MF transmission is delayed according to the characteristics of the ground over which it is traveling [8, 9]. These so-called Additional Secondary Factors (ASFs) must be taken into account for positioning applications. While computer modelling tools can predict ASFs using databases of ground conductivity and topography, the quality of the prediction is typically insufficient for the desired positioning accuracy; the tools also do not describe the time varying nature of the ASFs. The current solution to ASFs involves surveying the area of interest to account for spatial effects based upon topography and ground conductivity and establishing monitor sites (with appropriate communications links) to provide temporal corrections to account for the time variation in the delay [10].
- Finally, MF transmissions can suffer from multipath interference due to signal reflections off of the ionosphere; this is referred to as skywave interference [11] and the effect is most pronounced at night. While pulsed signals (such as Loran) can mitigate this effect, continuous transmission (as in MF R-Mode) will always suffer from it; the result is limited coverage range for each transmitter.

3. PROTOTYPE TRANSMITTER

To implement the CW version of DGNSS R-Mode a new modulator/transmitter is necessary:

1) While the legacy DGNSS transmissions have a specification of time stability [12], precise timing of the transmitted signal is key to accuracy in a pseudo-range-based positioning system; hence, a very stable (e.g. rubidium) clock and a UTC time base with 50 nsec synchronization accuracy are required at each transmission site.
2) Both the MSK and CW signals must be created at the transmitter site. This could be accomplished with a new, integrated modulator or the analog combining of low-level RF signals from a legacy MSK modulator and signal generators for the CW signals. In the second approach, the signal generators must be able to use precise clock and UTC synchronization signals in creating the CW.
3) The transmitter (amplifier) must be able to accommodate the resulting non-constant amplitude signal.
4) The antenna/coupler must be able to accommodate the wider bandwidth signal.

Figure 2 contains a basic block diagram of this modulator/transmitter system. For the testing described in this paper, both routes mentioned in item 2 above were employed to establish R-Mode transmit sites:

- A custom transmitter was constructed by Novator Solutions (Sweden). The unit accepts 10 MHz and 1 pulse per second (PPS) signals for synchronization and allows for adjustment of the relative and absolute power levels in the MSK and CW signals (see Figure 3). It also was designed so that the CW frequencies can be varied in 1 Hz increments.
- The signal was also created using a standard MSK modulator, two high-quality signal generators, and an RF combiner.

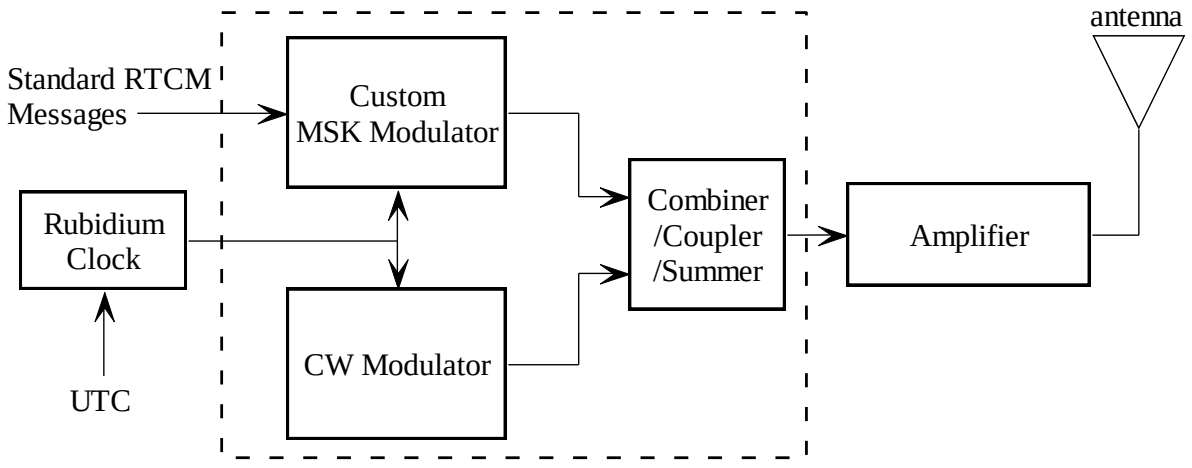

Figure 2: Block diagram for a prototype R-Mode transmitter.

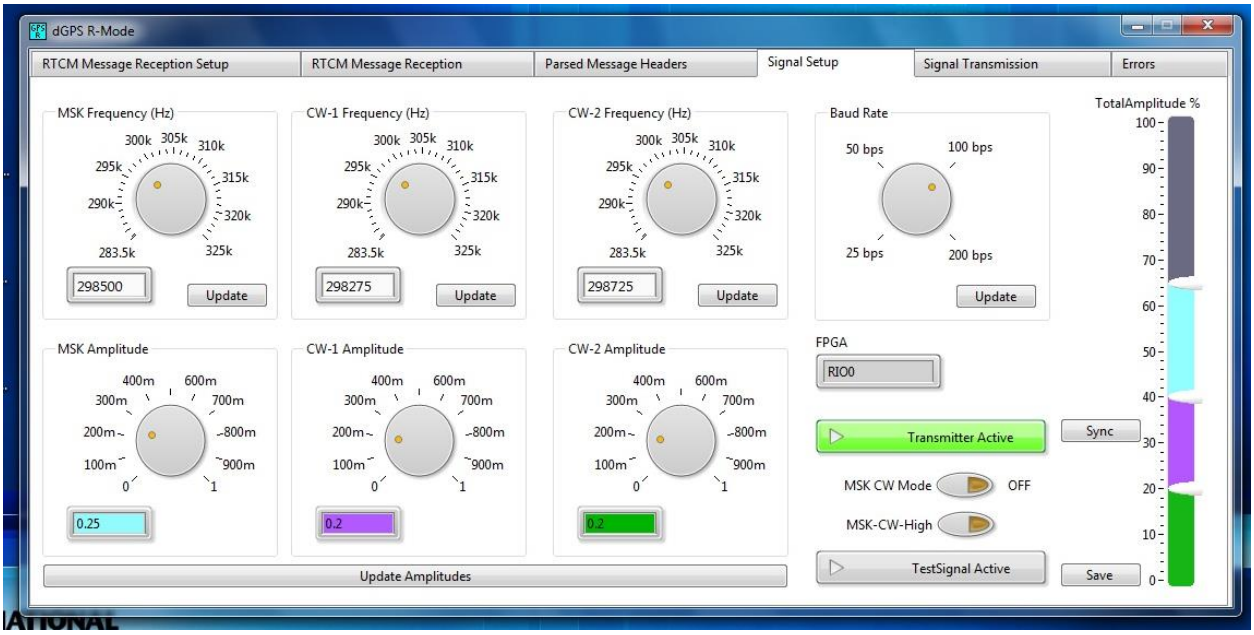

Figure 3: System configuration screen for Novator modulator.

4. PROTOTYPE RECEIVER

4.1. Receiver Overview

Figure 4 is a functional block diagram of the 2-channel MF R-Mode receiver. At this time only two channels are implemented so a position may only be acquired in range mode (requires clock synchronization). The receiver consists of the following:

- An analog DGNSS-band front end (filter and amplifier) is used to reduce out-of-band noise and interference due to signals in the adjacent low frequency (LF) and amplitude modulation (AM) bands. While a constant time delay is acceptable as it is removed in a trilateration solution, it is important that this analog front end not introduce *different* time delays for the different DGNSS channels.
- An analog-to-digital converter (ADC) sufficiently fast so as to record the entire DGNSS band as one signal is needed for synchronous signal processing (currently a 1 MHz sampling rate is used). A stable (e.g. rubidium) clock and a UTC time base allow this ADC to precisely collect the MF R-Mode data.
- A standard MSK demodulator (software block) that decodes RTCM messages.
- A CW phase estimator (software block) that implements the standard algorithm for the phase of the two transmitted CW signals on each channel.
- Finally, the ranges from each DGNSS channel and their associated weights are combined into a position solution. The output is a standard NMEA message.

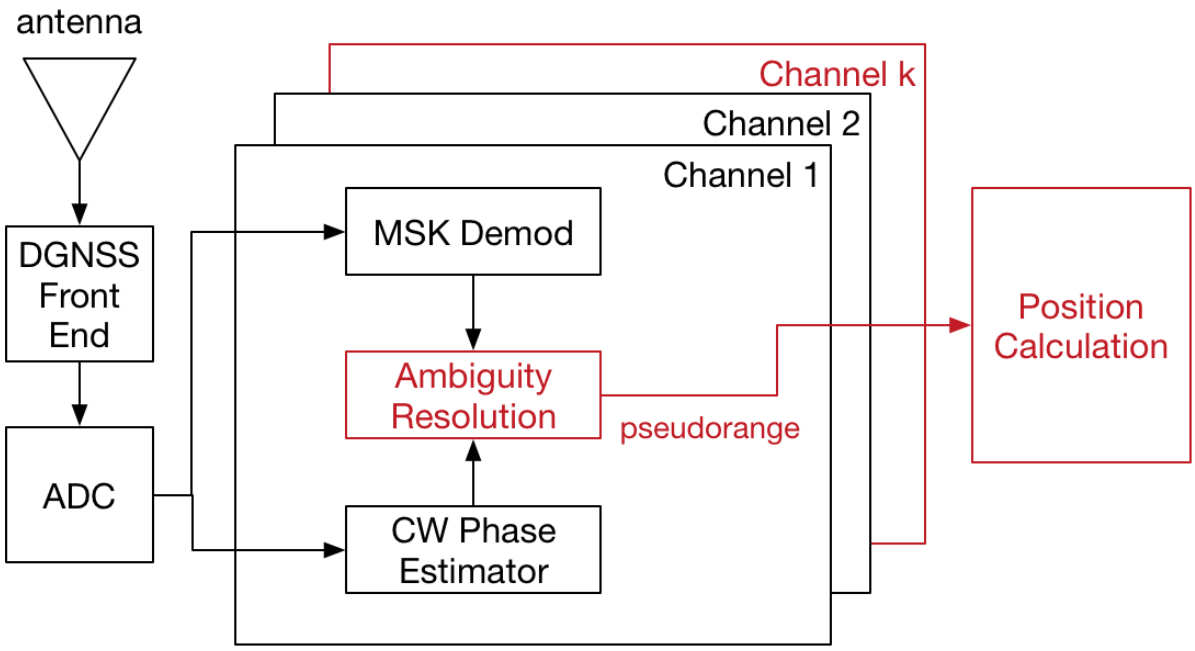

Figure 4: A prototype R-Mode receiver. The portions in red are not yet implemented.

The current prototype receiver demodulates the MSK transmission and estimates the phase angles of the two R-Mode CW signals for two DGNSS channels. The receiver does not resolve the cycle ambiguities, nor does it trilaterate to find the receiver's position (a range mode position is calculated using the two signals but the solution is very sensitive to any clock bias). Likewise, there are no ASF corrections in the current prototype solution. The algorithm employed is the standard phase estimator for sinusoids in white noise; details on the processing appear in Appendix A. Currently a 5-second block of data is read in and used to estimate the phase. This value was chosen so as to yield moderate phase accuracy (longer data records yield better estimates) while also limiting impacts on accuracy of a moving receiver (any motion over the processing period smears the phase estimate).

4.2. Receiver Software

The ranging receiver (2 channel) is implemented in MATLAB software; the processing chain is shown in Figure 5. The receiver software is supplied as a MATLAB executable program that is designed to run on a computer with an Adlink analog-to-Digital (A/D) board installed. To enable MATLAB to access the digital data from the A/D board the Adlink driver and software must also be installed. The antenna and analog filtering and amplification are discussed in the receiver manual. The software usage is described in detail in the Software User Manual.

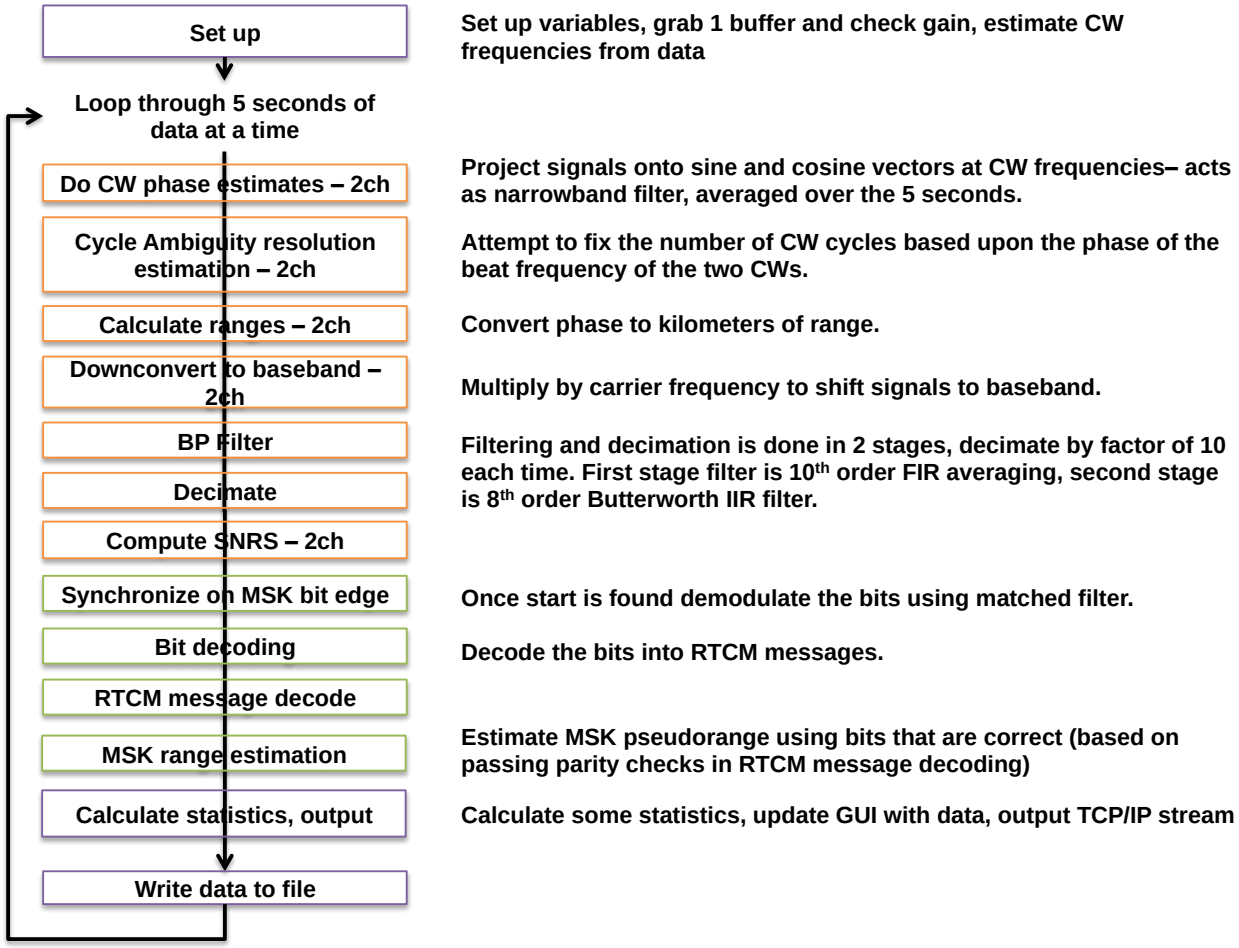

Figure 5: Software processing chain.

4.3. Position Solution

In order to convert two or three range measurements into a position solution, we assume:

- The transmitter locations are known.
- The receiver location is approximately known so that the CW cycle ambiguity is perfectly resolved.

The approach, as is typical of GNSS or Loran trilateration, is to linearize the range equations at a point near the actual position and to iteratively solve the equations in a least squares sense. For ground-based systems, since the different range estimates are of different precisions, this least squares solution usually includes weights based on the individual measurements' accuracies.

Specifically, for a presumed position solution $(\mathrm{e}_0, \mathrm{n}_0)$ parameterize the kth (of m) R-Mode signal as follows (e and n being east and north, respectively):

- r_k is the propagation distance from transmitter k to (e_0, n_0) measured in meters.
- θ_k is the bearing to transmitter k from (e_0, n_0).
- $\widehat{r_k}$ is the estimated range from transmitter k to the receiver.

- σ_k^2 is the variance of $\widehat{r_k}$ (and the $\widehat{r_k}$ are assumed to be independent random variables).

Defining the differentials for both position and the ranges

$$\delta_n = n\text{-}n_0 \qquad \delta_e = e\text{-}e_0 \qquad \delta r_k = \widehat{r_k}\text{-}r_k \;\; ; k = 1, \ldots m$$

the linearized range equations are

$$\begin{bmatrix} \delta r_1 \\ \delta r_2 \\ \vdots \\ \delta r_m \end{bmatrix} = \begin{bmatrix} \cos\theta_1 & \sin\theta_1 \\ \cos\theta_2 & \sin\theta_2 \\ \vdots & \vdots \\ \cos\theta_m & \sin\theta_m \end{bmatrix} \begin{bmatrix} \delta_n \\ \delta_e \end{bmatrix} = \mathbf{G} \begin{bmatrix} \delta_n \\ \delta_e \end{bmatrix}$$

Note that the resulting trigonometric matrix, the direction cosines **G**, is of a slightly different form (i.e. is missing a column of ones) than is usual for GNSS or Loran trilateration in that the current formulation employs synchronized clocks (recall that we are measuring ranges, not pseudoranges).

Since the range measurements for ground based (pseudo-)range systems are not of the same quality, it is common to solve the range equations in a weighted least squares sense. Assuming weights inversely proportional to the accuracy of each range

$$\mathbf{W} = \text{diag}\left(\frac{1}{\sigma_1^2}, \frac{1}{\sigma_2^2}, \ldots \frac{1}{\sigma_m^2}\right)$$

then the solution is

$$\begin{bmatrix} \delta_n \\ \delta_e \end{bmatrix} = (\mathbf{G}^T \mathbf{W}\, \mathbf{G})^{-1} \mathbf{G}^T \mathbf{W} \begin{bmatrix} \delta r_1 \\ \delta r_2 \\ \vdots \\ \delta r_m \end{bmatrix}$$

which allows for iteration of the new position

$$n_1 = n_0 + \delta_n \qquad e_1 = e_0 + \delta_e$$

Typically, one iterates these equations a few times until the solution converges. The resulting error covariance matrix is

$$(\mathbf{G}^T \mathbf{W}\, \mathbf{G})^{-1}$$

5. ANALYSIS OF TEST DATA

At night MF broadcasts can suffer from multipath interference due to signal reflection off of the ionosphere, so-called skywave; Figure 6(left) shows a simplified view of this reflection. We note:

- The skywave signal appears *later in time* than the ground wave signal (on the order of 100's of μsec later) since the propagation path is longer. Figure 6 (right) shows the typical time delays observed versus distance from the transmitter for a one-hop skywave (this is simply based upon the difference in the lengths of the two paths).
- The combination of the direct path plus skywave can cause considerably larger variation in the phase estimate with lower correlation between the two CW frequencies. Theoretically the skywave appears to be another CW signal, of the same frequency, but with different amplitude and phase. Such signals can add constructively or destructively (called fading), and can greatly impact the accuracy of the phase measurement.
- Skywave impacts are larger at further distances from the transmitter since the ground wave experiences higher attenuation than does the skywave; the relative signal powers are measured as a fade margin on a dB scale (ground wave minus skywave power), which can go negative (i.e. the skywave being stronger than the ground wave) [13].

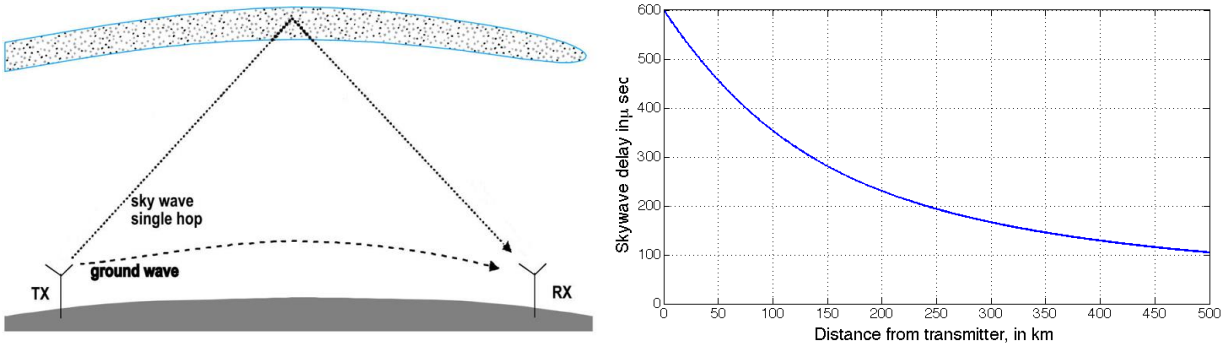

Figure 6: Skywave: left – a simplistic geometrical model; right – the time delay for this model (90 km ionospheric height) versus distance from the transmitter.

5.1. Skywave Impact on Ranging

To limit the impacts of noise and skywave on ranging accuracy, it is clear that a short operating range for MF DGNSS R-Mode is preferred; toward this end the ranges for the "shake-down" testing of the prototype transmitter and receiver along the Dutch coast were on the order of 25-50 km. While the density of DGNSS transmitters in the North Sea area is high, trilateration solutions will still require accurate estimation of pseudoranges out to 150 or, perhaps, 200 km. To assess the performance at such typical distances the MF DGNSS R-Mode transmitter was relocated to Heligoland, an archipelago off of the German coast in the North Sea (see Figure 7) and three receiver locations were chosen: Terschelling (213 km from the transmitter), the East end of the Kiel Canal (130 km), and Tönning (66 km).

Figure 7: Location of the transmitter (red) and three receivers (blue).

5.1.1. Summer Data

Some data was collected from the first two sites (Kiel Canal and Terschelling) in May (beginning of Summer). Figure 8 shows the SNR values over a 5-day period (27-31 May 2016) for the CW1 signal as received at the two sites. For clarity, the 5-second data samples have been filtered and decimated into data points every 5 minutes. The SNRs for Terschelling are 8-9dB lower, but it is also 90 km farther away. The green lines on this and in the next two figures indicate sunrise and the cyan lines indicate sunset. There was a large drop in the SNRs on both sites starting at ~1600 on 30 May, that lasted for about 8 hours. Since it is common to both sites, there may have been an issue at the transmitter. In this figure and the next two, only data from CW1 is examined as the data from CW2 is virtually identical (it is spaced only 450 Hz away and at the same power).

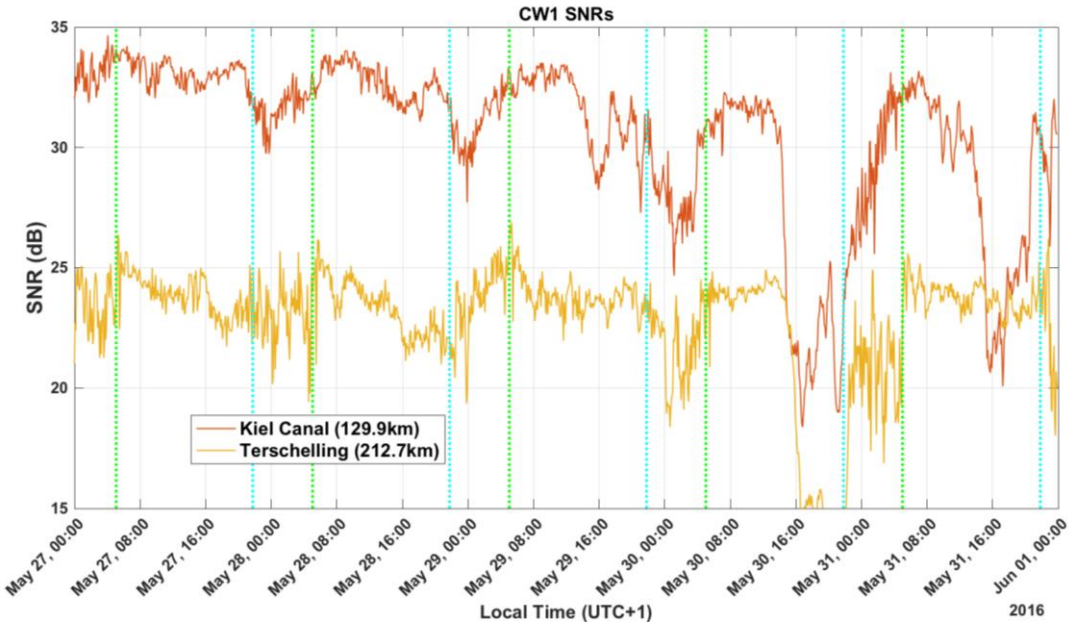

Figure 8:SNR values for CW1 for two sites, 27-31 May 2016.

The stability and quality of the phase measurements can be seen in Figure 9. In this figure, the raw phase measurements have been converted to meters and are shown relative to the mean value. Again the 5-second data samples have been filtered and decimated to 5-minute samples. In order to improve readability, the lines for Kiel and Terschelling have been offset by 40 and 100 meters, respectively. Both receive sites exhibit more noise in the phase measurements during the night (between the green and cyan lines), which is expected due to the skywave propagation; however, this is more obvious in the longer signal paths of the Terschelling data. The impact of this increase in noise is quantified in Figure 10, which shows the standard deviations in the phase measurements versus time (note that these are 1-sigma values). Each data point in Figure 10 is the standard deviation of the previous 1-hour of samples (nominally 720 5-second intervals). During the day, the standard deviations are in the 1-3 m range for the closer site and 2-5 m for the more distant site. At night due to the impact of skywave, the values increase to 10-35 m for the closer site, and up to 40 m or so for the farthest site. The averages of the standard deviation across all of the day (sunrise to sunset) and night periods are shown in Table 1.

Table 1: Average Standard Deviations for Day and Night, May.

	Average Standard Deviation (m)	
Site	**Day**	**Night**
Tönning		
Kiel Canal	1.4	13.9
Terschelling	3.6	18.8

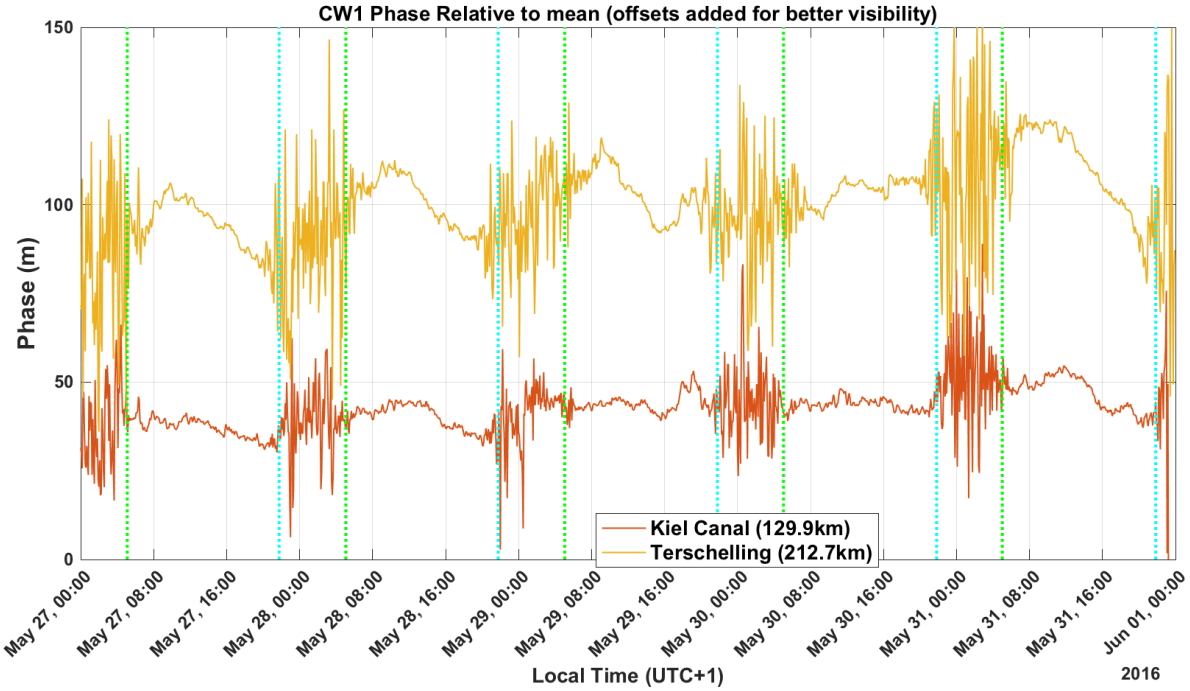

Figure 9: CW1 phase estimates for the two sites over the period 27-31 May. Phase is in meters relative to the mean, with offsets added to Kiel Canal and Terschelling to improve readability of the graphs.

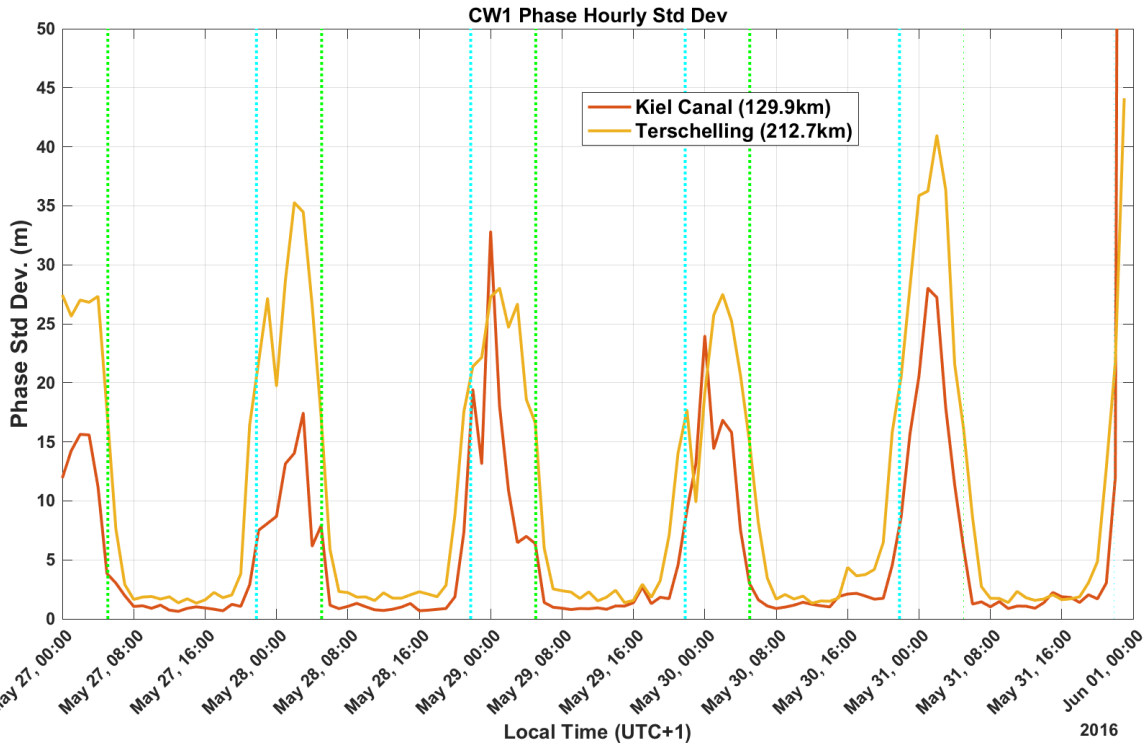

Figure 10: Standard deviation on phase measurements for both receiver sites, 27 – 31 May.

5.1.2. Winter Data

During the winter (Dec 2016) some additional data was captured from the original two sites plus the new site at Tönning. Again, only data from CW1 is examined as the CW2 data is virtually identical. Figure 11 shows the SNR values over a 4-day period (1-4 Dec 2016) for the CW1 signal as received at each of the three sites. As before, the 5-second data samples have been filtered and decimated into data points every 5 minutes. The SNRs for Tönning and the Kiel Canal are similar at night; during the day, it appears that there is some local interference source that lowers the SNR by about 3 dB at Tönning. The noise source started later on December 3rd (Saturday) and was not present on the 4th (Sunday) so is probably a work-related noise source. As in the previous figures, the green lines on this and in the next two figures indicate sunrise and the cyan lines indicate sunset.

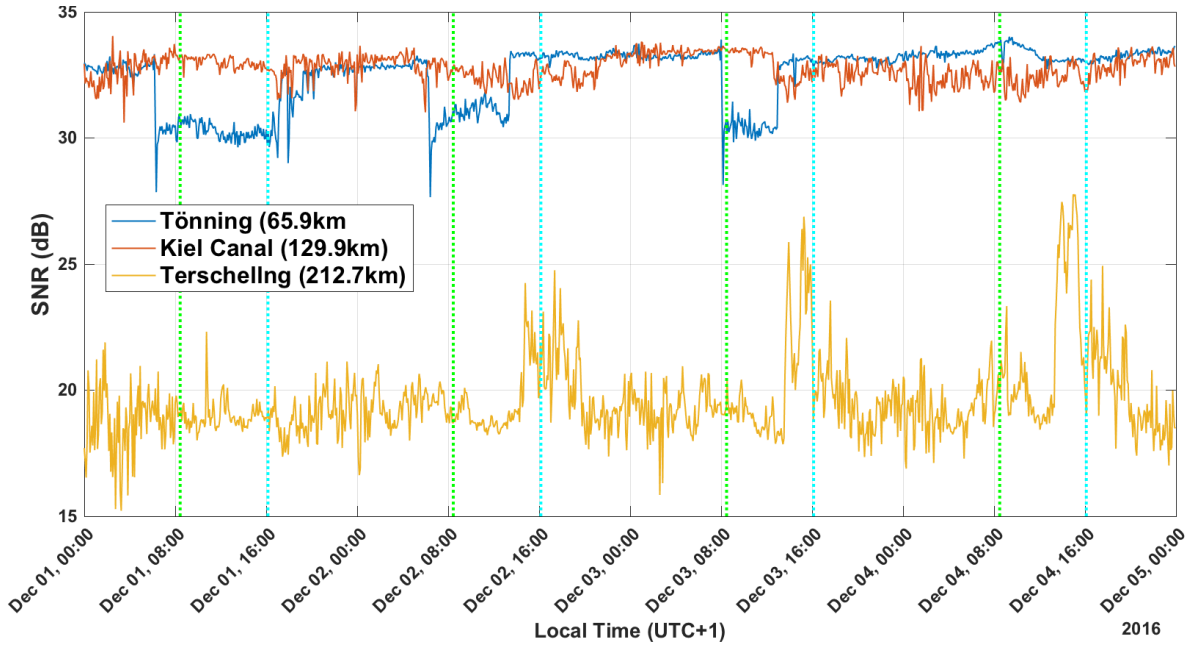

Figure 11: SNR values for CW1 for all three sites, 1-4 Dec.

The stability and quality of the phase measurements can be seen in Figure 12. In this figure, the raw phase measurements have been converted to meters and are shown relative to the mean value. Again the 5-second data samples have been filtered and decimated to 5-minute samples. In order to improve readability, the second and third lines have been offset up from the first (by 40 and 100 meters, respectively). All three receive sites exhibit more noise in the phase measurements during the night (between the green and cyan lines), which is expected due to the skywave propagation; however, this is much more obvious in the longer signal paths of the Terschelling data. The impact of this increase in noise is quantified in Figure 13, which shows the standard deviations in the phase measurements versus time (note that these are 1-sigma values). Each data point in Figure 13 is the standard deviation of the previous 1-hour of samples (nominally 720 5-second intervals). During the day, the standard deviations are in the 2-3 m range for the two closer sites and 5-10 m for the more distant site. At night, due to the impact of skywave, the values increase to 4-10 m for the closest site, and from 10-20 m for the midrange site, and up to 40 m or so for the farthest site. The averages of the standard deviation across all of the day (sunrise to sunset) and night periods are shown in Table 2.

Table 2: Average Standard Deviations for Day and Night, December.

	Average Standard Deviation (m)	
Site	**Day**	**Night**
Tönning	2.3	4.3
Kiel Canal	3.1	10.7
Terschelling	7.1	20.5

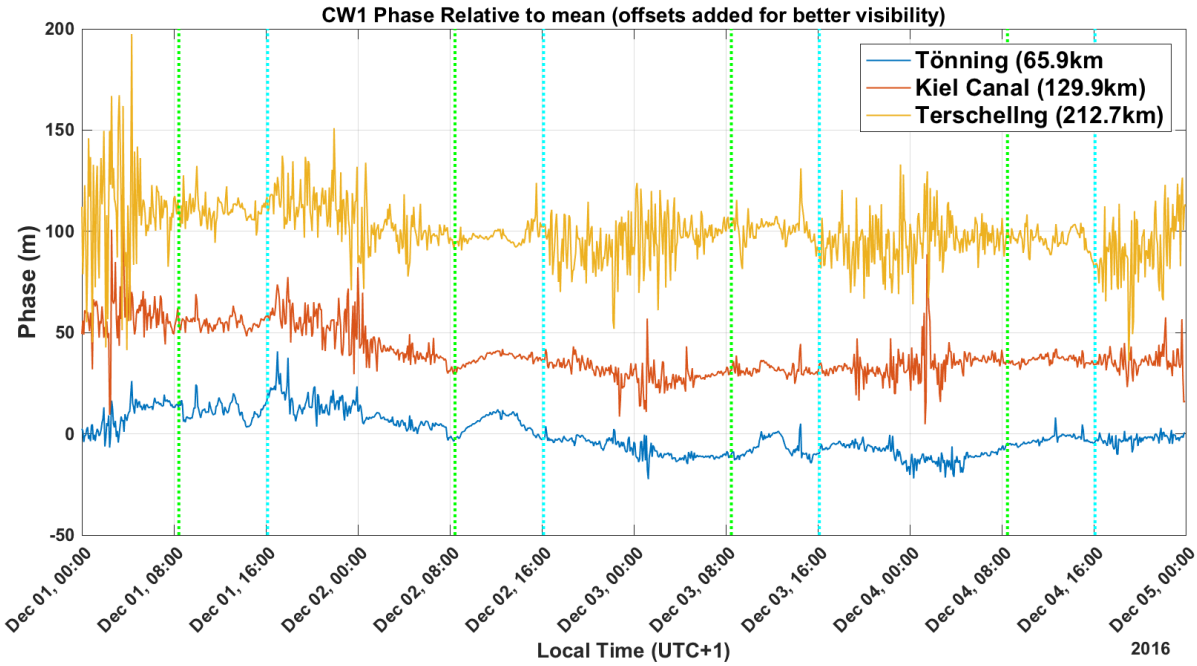

Figure 12: CW1 phase estimates for each site over the period 1-4 Dec. Phase is in meters relative to the mean, with offsets added to Kiel Canal and Terschelling to improve readability of the graphs.

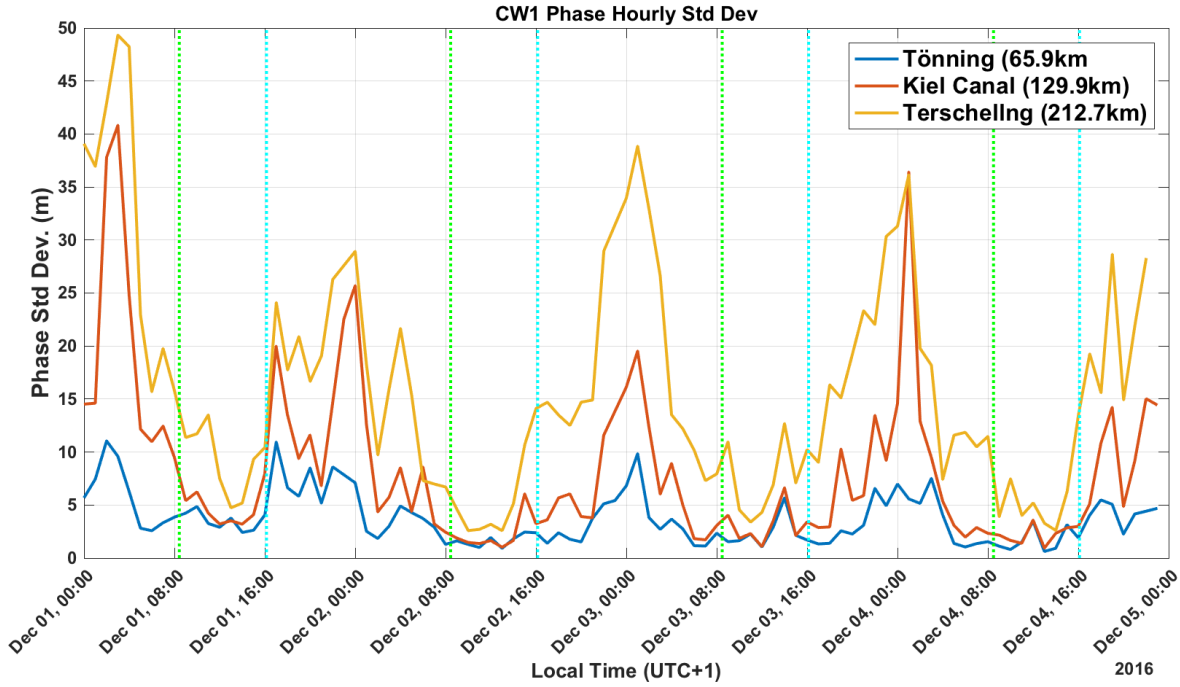

Figure 13: Standard deviation on phase measurements for each of the three receiver sites, 1-4 Dec.

This skywave impact can be seen in the much larger standard deviations at night in Figure 13. These values increase the most at night for the farthest stations (see averages in Table 2). However, in all cases these standard deviations are small enough to allow for trilateration-based positioning. The decrease in SNR did not seem to impact performance appreciably.

5.1.3. Data sets compared

During the winter of course, the nights are longer, so the periods of worse performance due to nighttime skywave are longer. This can be seen in Figure 14; the December data is the dashed lines, and for the two sites that there is May data (solid lines) the shorter durations of skywave impact are clear. There is insufficient data to really assess whether the phase standard deviations are really different in summer vs. winter. The data in Tables 1 and 2 is inconclusive, but is only for 4 days.

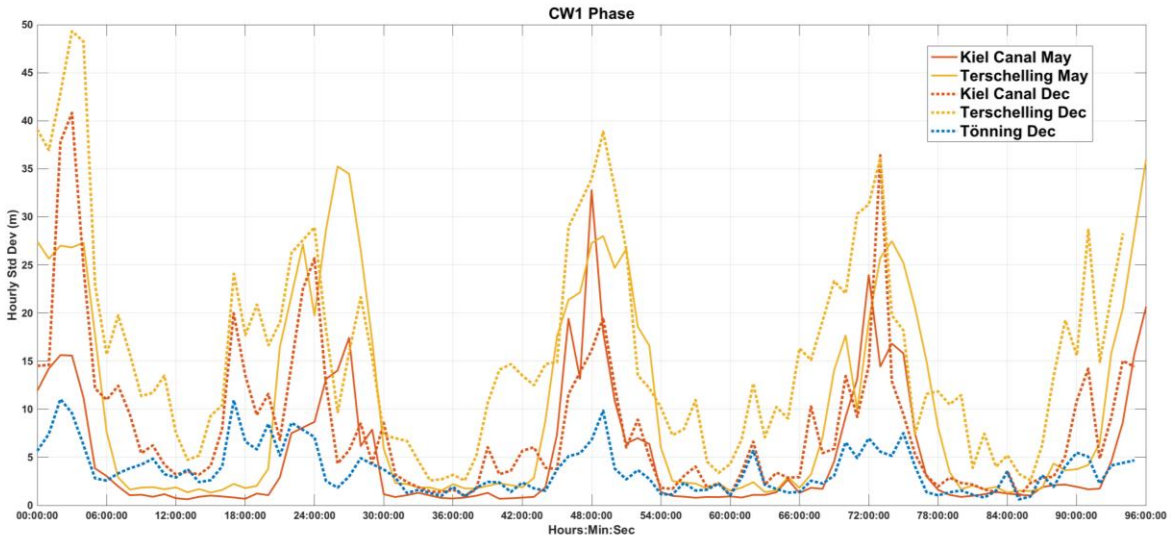

Figure 14: Hourly average standard deviation for the 3 sites in May and December.

In addition to the impact of the skywave, variations in the phase measurement over the course of the day can also be seen. The small scale variations in range experienced during the day (the range values appear to be wandering a bit) are likely due to weather induced fluctuations in the conductivity of the propagation path; similar temporal variation has been observed in 100 kHz Loran signals [10]. Also of note, is that the variation in the phase measurements is greater during the winter than in the summer; this same seasonal variation has been observed in Loran signals as well [14]. This can be seen in Figure 15 for the two sites that we have summer and winter data for. In addition, there seems to be some correlation among the sites in the seasonal/temporal variation in the phase. Figure 16 shows 96 hours of phase measurements for both sites in May and December. The May data (solid lines) trends the same as does the December data (dashed lines). This bodes well for positioning as common mode or correlated changes in the phase measurements will drop out in the position solution.

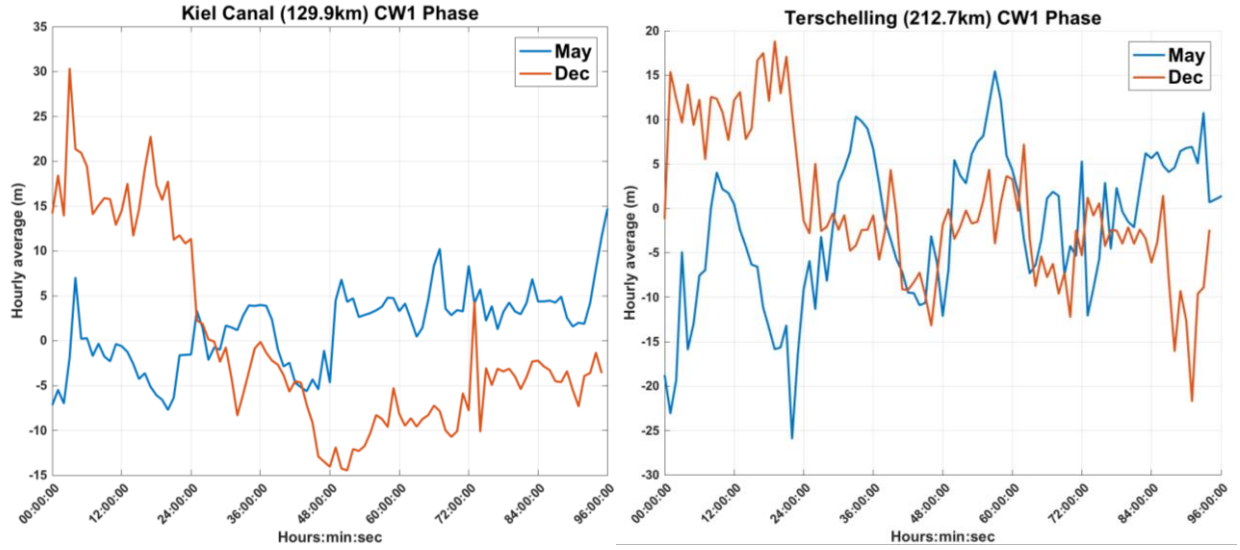

Figure 15: Kiel Canal (left) and Terschelling (right) hourly average phase measurements, May and December.

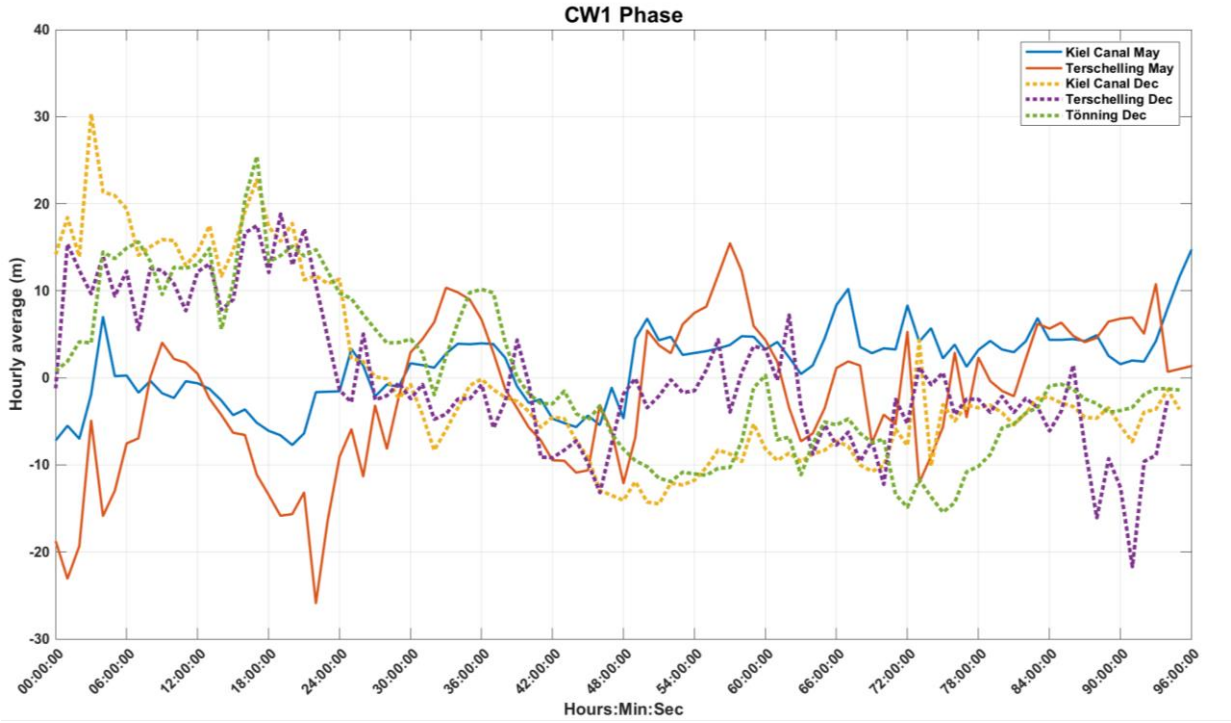

Figure 16: Hourly average phase measurements for three sites, May and December.

5.2. Simulated Positioning Performance

As the R-Mode project develops, it is of interest to assess the positioning performance that would be achieved; unfortunately, positioning is not possible with a single transmitter. However, we can consider the experiment in which we reverse the roles of the transmitter and receivers; specifically, solving for the "unknown" transmitter's location based upon the range measurements and the "known" locations of the three receivers.

The data for this experiment is actual ranges, equal to the measured phase plus an integer number of wavelengths of the CW so that, on average, the range is accurate for the known locations. The solution method is an iterative least squares solution of the range equations (similar to the trilateration solution method for Loran or GPS, but assuming that the clock offset term is zero). Unfortunately, the dilution of precision (DOP) for the actual receiver locations is quite high (>30!) and the solved positions would have a very strong north-south scatter; hence, for this experiment, the "location" of the Kiel Canal site was rotated to be due south of Heligoland, but at the same distance, to improve the geometry and reduce the DOP (see Figure 17).

The performance of such an experiment is shown in Figure 18 using a portion of the range data from Figure 12. The left subfigure shows the error scatter for a 6-hour period during the day; we note the tight scatter and the small 95% (2-sigma) error radius. The right subfigure shows the error scatter for a 6-hour period during the night, during a period with large range variation; although the error scatter has grown, its 95% (2-sigma) error radius is still quite reasonable.

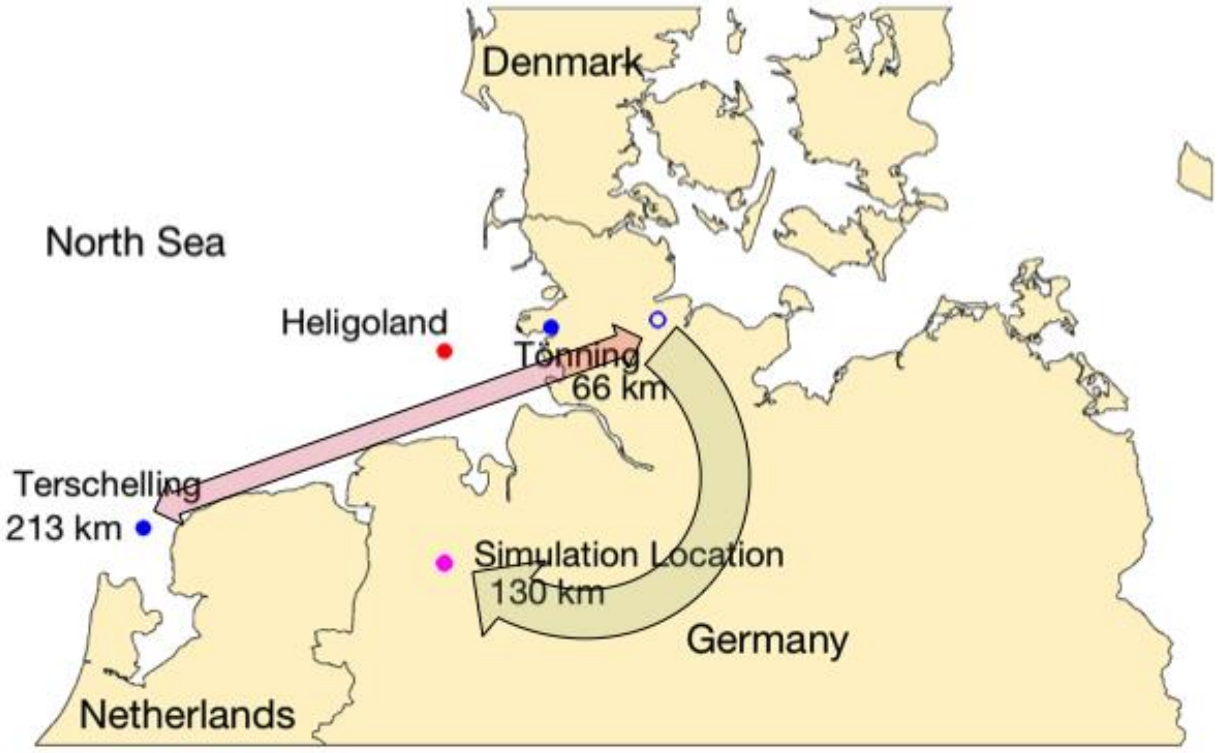

Figure 17: Sites used for the position simulation.

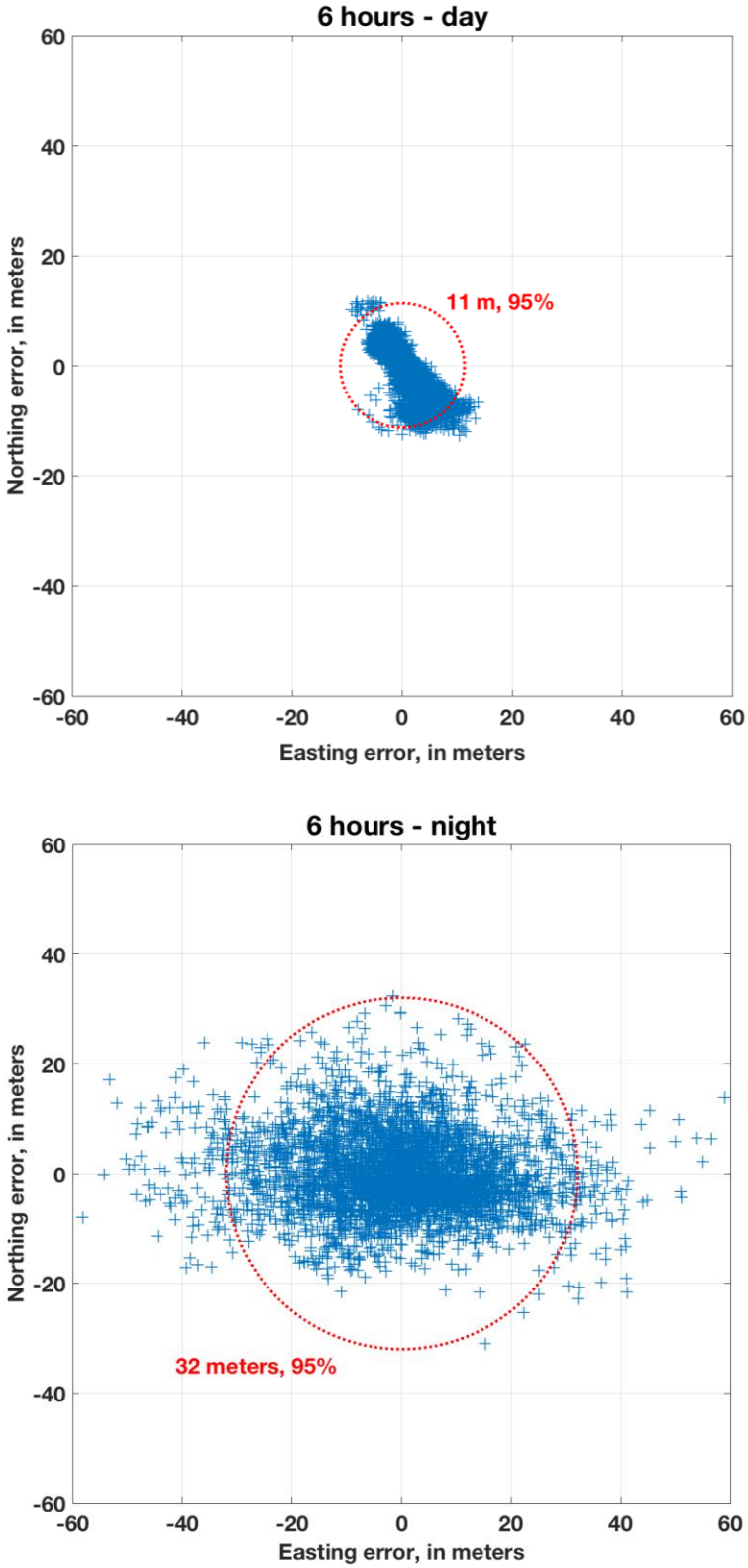

Figure 18: Performance of the simulated positioning experiment. The red circle is the 95% error radius.

6. CONCLUSIONS

Investigations to date bear out the predictions of the Feasibility Study [6] and suggest that the phase of the CW signals can be tracked well enough to yield good positioning performance out to 200 km. During the day, the performance of all three ranges is better than 10 m, while at night, due to the influence of skywave, the performance decreases, but is still around 20m or less (the Feasibility Study assumed a night time performance an order of magnitude worse than the daytime performance). The positioning performance predicted by our data appears to be on the order of 11m 2DRMS during the day and 32m 2DRMS at might. Whether the achievable performance level is acceptable or not for a back-up system needs to be determined by the Competent Authority.

The propagation speed of ground wave signals such as the proposed R-Mode CW vary during the course of the day and season; this temporal ASF effect is visible in the current data and has been previously noticed with Loran signals at 100 kHz. Such temporal effects can be dealt with by using reference stations to track the variations, transmitting “corrections” on the MSK signal or some other augmentation channel.

7. FUTURE WORK

In order to develop and test positioning receivers, additional R-Mode transmitters are needed; two for ranging mode and three for pseudorange mode. The WSV has already set up a 2nd transmitter (at Zeven), which will enable experiments with ranging modes. Hopefully a third will soon follow to allow testing of pseudorange mode. In addition, works needs to be done developing and testing cycle ambiguity resolution procedures for the CW phase as to date, this has been assumed to be fixed. Additionally, work needs to be done to estimate the impact of the ASF temporal variations in order to determine the required number of reference stations. We note that the density of DGNSS transmitters in ITU Region I suggests co-locating the reference stations with the transmitters. It also appears likely that the spatial ASF variation can be ignored due to the short ranges to the transmitters.

8. REFERENCES

[1] J. Raquet. (2006, August) Navigation Using Signals of Opportunity. *GPS World Discussion Forums*.

[2] G. W. Johnson and P. F. Swaszek, "Feasibility Study of R-Mode using MF DGPS Transmissions," German Federal Waterways and Shipping Administration, Milestone 2 Report, 11 March 2014.

[3] G. Johnson, P. Swaszek, J. Alberding, M. Hoppe, and J.-H. Oltmann, "The Feasibility of R-Mode to Meet Resilient PNT Requirements for e-Navigation," in *ION GNSS Conference*, Tampa, FL, 2014.

[4] S. Pasupathy, "Minimum Shift Keying: A Spectrally Efficient Modulation," *IEEE Communications Magazine,* vol. 17, pp. 14-22, 1979.

[5] J. F. Kasper and C. E. Hutchinson, "The Omega navigation system--An overview," *Communications Society Magazine, IEEE,* vol. 16, pp. 23-35, 1978.

[6] G. W. Johnson and P. F. Swaszek, "Feasibility Study of R-Mode combining MF DGNSS, AIS, and eLoran Transmissions," German Federal Waterways and Shipping Administration, Final Report, 25 September 2014.

[7] G. Frenkel and D. Gan, "Ambiguity Resolution in Systems Using Omega for Position Location," *IEEE Transactions on Communications,* vol. 22, pp. 305-312, 1974.

[8] N. DeMinco, "Medium Frequency Propagation Prediction Techniques and Antenna Modeling for Intelligent Transportation Systems (ITS) Broadcast Applications," U.S. Dept. of Commerce NTIA Report 99-368, August 1999.

[9] N. DeMinco, "Propagation Prediction Techniques and Antenna Modeling (150 to 1705 kHz) for Intelligent Transportation Systems (ITS) Broadcast Applications," *IEEE Antennas and Propagation Magazine,* vol. 42, p. 26, August 2000.

[10] G. W. Johnson, P. F. Swaszek, R. Hartnett, R. Shalaev, C. Oates, D. Lown*, et al.*, "A Procedure for Creating Optimal ASF Grids for Harbor Entrance & Approach," presented at the ION GNSS 2006, Fort Worth, TX, 2006.

[11] *ITU-R Handbook on the Ionosphere and its Effects on Radiowave Propagation*. Geneva: ITU-R, 1998.

[12] "Broadcast Standard for the USCG DGPS Navigation Service," U.S. Coast Guard, Washington, DC COMDTINST M16577.1, April 1993.

[13] D. C. Poppe, "Coverage and Performance Prediction of DGPS Systems Employing Radiobeacon Transmissions," PhD. Dissertation, University of Wales, Bangor, UK, 1995.

[14] G. Johnson, P. Swaszek, R. Hartnett, K. Dykstra, and R. Shalaev, "Temporal Variation of Loran ASFs and their Effects on HEA Navigation," presented at the ENC 2008, Toulouse, France, 2008.

[15] D. Rife and R. R. Boorstyn, "Single tone parameter estimation from discrete-time observations," *Information Theory, IEEE Transactions on,* vol. 20, pp. 591-598, 1974.

[16] D. C. Rife and R. R. Boorstyn, "Multiple Tone Parameter Estimation from Discrete-Time Observations," *Bell Systems Technical Journal,* pp. 1389 - 1410, November 1976.

[17] S. M. Kay, *Fundamentals of Statistical Signal Processing, Volume I: Estimation Theory*: Prentice Hall, 1993.

APPENDIX A. RANGE ESTIMATE FROM THE CW

For simplicity, consider just the CW portion of the broadcast and write the received signal as the sum of the transmitted CW (frequency f_m) and noise

$$r(t) = A\cos 2\pi f_m(t\text{-}\tau) + w(t)$$

In this expression, A is the received amplitude and τ accounts for the propagation delay (nominally equal to d/c, d being the range from the transmitter and c the speed of light, plus factors pertaining to speed of propagation and channel effects); $w(t)$ is the noise, assumed to have variance σ^2. Converting to phase angle, this received signal is

$$r(t) = A\cos(2\pi f_m t + \theta) + w(t)$$

in which $\theta = 2\pi f_m \tau$. In other words, the propagation delay is manifested as a phase shift and, because of the periodic nature of the sine function, the range can only be estimated with an ambiguity dependent upon the wavelength of the sinusoid (approximately 1 km for the MF DGNSS band).

Estimating the phase in such a situation is well understood; relevant references include Rife [15, 16] and Kay [17]. Sampling every T_s seconds we have the data sequence

$$r[n] = A\cos(2\pi f_m n T_s + \theta) + w[n]$$

for $n = 0, 1, \ldots N-1$ and are interested in estimators $\hat{\theta}$ for the unknown phase. A lower bound to the variance of any unbiased estimate is the Cramer-Rao Bound (CRB). For the sampled version of this problem this is

$$\mathrm{Var}(\hat{\theta}) \geq \frac{2\sigma^2}{A^2 N}$$

Noting that the signal to noise ratio, SNR, for this signal is $\mathrm{SNR} = \frac{A^2}{2\sigma^2}$, then the CRB is $\mathrm{Var}(\hat{\theta}) \geq \frac{1}{N\ \mathrm{SNR}}$ and the variance decreases as both N and the SNR increase (as would be expected).

The maximum likelihood estimate (MLE) of θ involves projecting the received signal onto both the sine and cosine functions of the same frequency and using the arc-tangent function (on the full 0 to 2π range) to recover θ

$$\hat{\theta}_{MLE} = \text{-}\,\mathrm{atan}\left(\frac{\sum_{n=0}^{N-1} x[n]\sin 2\pi f_m n T_s}{\sum_{n=0}^{N-1} x[n]\cos 2\pi f_m n T_s}\right)$$

We note:

This estimator is asymptotically efficient in that as N goes to infinity then the distribution of the estimate converges to a Gaussian density with mean equal to the true phase and variance equal to the CRB.

The MLE of the range (without solution of the ambiguity) is this phase estimate transformed to distance using the wavelength of the sinusoid

$$\hat{r}_{MLE} = -\frac{c}{2\pi f_m} \operatorname{atan}\left(\frac{\sum_{n=0}^{N-1} x[n] \sin 2\pi f_m n T_s}{\sum_{n=0}^{N-1} x[n] \cos 2\pi f_m n T_s}\right)$$

For two CW signals in white noise the joint MLE is just the pair of separate MLEs.